Contribution from the Departments of Chemistry, Yale University, New Haven, Connecticut 06511-8118, Oklahoma State University, Stillwater, Oklahoma 74078, and Manhattanville College, Purchase, New York 10577

Inter- vs. Intramolecular C-H Activation: A C-H-Ir Bridge in $[IrH_2(8\text{-methylquinoline})L_2]BF_4$ and a C-H + M → C-M-H Reaction Trajectory

ROBERT H. CRABTREE,*† ELIZABETH M. HOLT,*‡ MARYELLEN LAVIN,† and SHEILA M. MOREHOUSE§

Received October 26, 1984

The complexes $[IrH_2L'(PPh_3)_2]A$ (L' = 8-methylquinoline, caffeine) each contain a C-H···Ir bridge, structurally characterized in the methylquinoline case (A = SbF_6). The complex is monoclinic, space group $P2_1/n$ with a = 19.221 (4) Å, b = 21.202 (11) Å, c = 11.079 (5) Å, β = 104.56 (3)°, and Z = 4. The final R factor was 4.6%. A structural measure of the strength of the bridging interaction was developed and used to systematize the data on this and 17 related structures. The results are used to construct a C-H + M → C-M-H reaction trajectory. On the basis of this trajectory, we propose that, for a given metal species capable of breaking C-H bonds, conformational and steric effects will play an important role in deciding whether cyclometalation or attack on external substrate such as an alkane will take place. In particular, it is suggested that sterically uncongested metal systems will favor the occurrence of alkane activation, rather than cyclometalation.

Introduction

In this paper we attempt to define more clearly the way in which metals break C-H bonds in reactions of the oxidative addition type (eq 1). These are believed to occur not only in the α- and

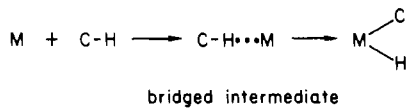

(1)

β-elimination processes but also in many alkane activation[1] systems. The dissection of the C-H bond is in each case accompanied by the formation of an M-C and an M-H bond.

A recent review by Brookhart and Green[2] covers complexes containing C-H···M bridges between a C-H bond of a ligand and the metal. They have called attention to the importance of these complexes, which they term "agostic", in relation to the general problem of C-H activation.

Two questions attracted our attention. First, why do C-H···M bridging groups exist at all in isolable systems? One might expect the C-H bond to be broken to give a C-M-H (cyclometalated) complex. Second, all the alkane C-H bond activation systems recently discovered[1] have C-H bonds in the ligands of the complex. Why does the metal not attack these C-H bonds, as might have been expected on the basis of the chelate effect, but rather those of the alkane? In both cases, the cyclometalation product is not seen, yet cyclometalation[3] is known to be a facile process, of which there are thousands of examples. Indeed, in planning our attack on the problem of alkane activation in 1978, we thought that we would first have to make metalation-resistant ligands[4] before progress could be made on the main problem. The fact that alkane activation systems containing PMe_3, C_5Me_5, and even PPh_3 work well, the cyclometalation product not being observed, is a surprising feature of this chemistry. Why this preference for inter- over intramolecular reaction is observed for these systems is a major unsolved question in C-H activation studies.

In our own alkane activation system,[5] based on $[IrH_2(Me_2CO)_2L_2]A$ (1: L = PPh_3, $(p\text{-}FC_6H_4)_3P$; A = BF_4, SbF_6), we had only been able to detect one intermediate, $[IrH(C_6H_7)L_2]SbF_6$ (2), in the dehydrogenation of cyclohexane to benzene, but we were able to obtain no direct evidence about the first step of the reaction: the first C-H bond cleavage. Morris[6] et al. have given good NMR spectral evidence for the presence in $[IrH(1,1,2\text{-trimethylallyl})L_2]BF_4$ of a methyl group bridged to the metal. Suggs[7] et al. have used 8-substituted quinolines as ligands to enable a close interaction to take place between the 8-substituent and the metal. We therefore decided to look at the 8-methylquinoline (mq) complex of 1 to see whether we could obtain some information about the critical first step in C-H activation in this iridium system. We report in this paper that 1 reacts with mq to give a complex $[IrH_2(mq)L_2]A$, which contains a bridged methyl group. The complex, which is also a catalyst for the selective deuteration of mq by D_2, has been characterized crystallographically. A detailed comparison of the C-H···M geometries for the 17 cases now known has allowed us to propose a detailed trajectory for the C-H + M → C-M-H reaction.

Results and Discussion

In order to test our expectation that mq might show significant C-H/metal interaction, we began by looking at its behavior with 1 and D_2. Catalytic deuteration was observed at the methyl group. Among a series of related ligands that we studied, mq and the

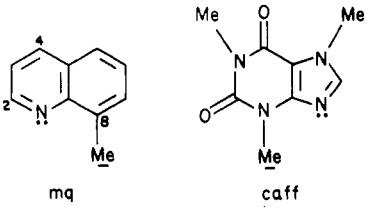

structurally similar ligand caffeine (caff) showed the most rapid deuteration. They are both deuterated by 1 at 25 °C under 1 atm of D_2, largely at the methyl groups (underlined in the diagrams) vicinal to the nitrogen (shown as N: in the diagrams) to which the metal binds. At a substrate:catalyst ratio of 20:1 and at 25 °C in CH_2Cl_2, exchange was half-complete in 90 min and essentially complete in 8 h, as judged by GC-MS. Apart from small isotope effects, simple statistics determine the final proportions of the various deuterated products, depending on the mole ratio of D_2:CH_3 of substrate. At a ratio of 0.5 the final deuteration was ca. 0.75 atom of D/mol of mq or caff. We never completely deuterated the substrates, but this could in principle be done by exposing them to successive aliquots of fresh D_2. In each case, we were able to show that the deuteration was predominantly (~95%) at the indicated vicinal methyl groups (see diagrams). ^1H and ^2H NMR showed that only these positions lost H and gained D. Some incorporation (~5%) also took place at the 2-position in mq.

2-Methylquinoline gave very slow ($t_{1/2}$ > 10 h) incorporation of D about equally into the methyl group and into the aromatic ring (presumably at the 8-position). 4-Methylquinoline only gave

† Yale University.
‡ Oklahoma State University.
§ Manhattanville College.

(1) Muetterties, E. L. *Chem. Soc. Rev.* **1983**, *12*, 283.
(2) Brookhart, M.; Green, M. L. H. *J. Organomet. Chem.* **1983**, *250*, 395.
(3) Bruce, M. I. *Angew. Chem., Int. Ed. Engl.* **1977**, *16*, 73.
(4) Anton, D. R.; Crabtree, R. H. *Organometallics* **1983**, *2*, 621.
(5) Crabtree, R. H.; Mellea, M. F.; Mihelcic, J. M.; Quirk, J. M. *J. Am. Chem. Soc.* **1982**, *104*, 107. Burk, M. J.; Crabtree, R. H.; Parnell, C. P.; Uriarte, R. J. *Organometallics* **1984**, *3*, 816.
(6) Howarth, O. W.; McAteer, C. H.; Moore, P.; Morris, G. E. *Chem. Commun.* **1981**, 506.
(7) Suggs, J. W. *J. Am. Chem. Soc.* **1978**, *100*, 640. Suggs, J. W.; Pearson, G. D. N. *Tetrahedron Lett.* **1980**, *31*, 3853.

0020-1669/85/1324-1986$01.50/0

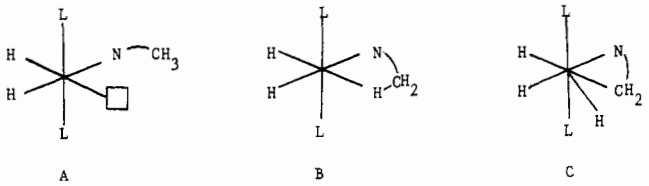

Figure 1. Possible structures for $[IrH_2(L')L_2]^+$ (L' = mq or caff) (NCH_3 = L', □ = empty site, counterion, solvent or H_2O): A, uncomplexed methyl group; B, C–H···M-bridged methyl group; C, methyl C–H completely dissected.

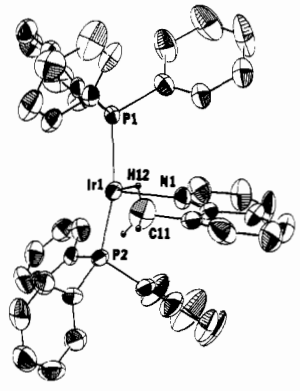

Figure 2. ORTEP diagram of the structure of the complex cation in **4a**, showing the bridging group C11–H12–Ir1.

a trace incorporation over 24 h, and 2,6-dimethylpyridine, 2,4,6-tri-*tert*-butylphenol, *o*-xylene, and methylcyclohexane gave no incorporation. Only trace incorporation was observed into the solvent or the PPh_3 groups of the catalyst.

Having identified mq and caff as the ligands showing the most rapid deuteration, we then studied their stoichiometric reaction with **1**. Complexes were formed, but it proved to be more convenient to make them by hydrogenation of $[Ir(cod)L_2]A$ (**3**) in the presence of the ligands. A CH_2Cl_2 solution of **3** reacts with 3 mol equiv of mq or caff at 0 °C to give the new complexes $[IrH_2(L')L_2]A$ (**4**: L' = mq (**a**) or caff (**b**); A = BF_4, SbF_6) (eq 2). Both materials were isolated as colorless prisms and were

$$[Ir(cod)L_2]^+ \xrightarrow{H_2,\ 0\ °C,\ L'} [IrH_2(L')L_2]^+ \qquad (2)$$

3 → **4a**, L' = mq; **b**, L' = caff

formulated as **4** on the basis of microanalytical and spectral data and by a crystallographic study of **4a**.

The chief point at issue is whether the exchangeable methyl group in **4** is uncomplexed (A), bridged (B), or completely dissected (C) as shown in Figure 1. In case A, the metal has only 16 valence electrons, an uncommon but not an unknown configuration for Ir(III). The "empty" site might even be occupied by the counterion, solvent, or perhaps even H_2O. Case B would be an 18-electron Ir(III) structure, a common configuration. Case C was also envisaged, even though the formal oxidation state would be Ir(V), rare but not impossible.

Fortunately, we were able to obtain definitive crystallographic evidence for structure B in the solid state. The data appear in Tables I–III and 1–3 (supplementary material), and a diagram of the structure is shown in Figure 2. The key piece of evidence is the distance from the metal to the carbon, C11, of the bridging methyl group: 2.69 (1) Å. This alone precludes structures A or C. A directly bonded CH_2Ar group (structure C) would have an Ir–C distance of ca. 2.1 Å.[8a] A nonbonded methyl would have a Ir···C distance of ca. 3.5 Å. The structure of $Pt(caff)_2Cl_2$,[9] in which the vicinal *N*-methyl group of the caffeine is believed *not* to be bridging, confirms this estimate, the Pt···C distance being 3.48 Å. Only the presence of an $ArCH_2$–H···Ir system can account for the observed distance.

Table I. Crystal Data for **4a**

formula	$C_{46}H_{41}F_6IrNP_2Sb$
mw	1097.7
a	19.221 (4) Å
b	21.202 (11) Å
c	11.079 (5) Å
α	90.0°
β	104.56 (3)°
γ	90.0°
V	4370.0 (31) Å^3
μ(Mo Kα)	42.88
λ(Mo Kα)	0.710 69 Å
D_{calcd}	1.668 g cm^{-3}
Z	4
F(000)	2144
no. of obsd reflcns	4749
R	4.6%
space gp	$P2_1/n$
color	colorless
octants collcd	$\pm h,+k,+l$

Electron density maxima, observed in the vicinity of the agostic (bridging) carbon, appear to be associated with the methyl hydrogens; they were successfully refined positionally as hydrogens. The observed bond lengths and angles are reasonable for a methyl group. One hydrogen, H12, is located in a bridging position between C11 and Ir. Ir–H12 and C11–H12 distances of 2.08 (10) and 0.96 (10) Å as well as the C11–H12–Ir angle of 119° were all reasonable and fall in the range of previously observed values[2] for other agostic systems. We defer further discussion of the C–H–M bridge to a later section.

The mq group is planar, and the Ir and C11 methyl groups are very close to the ideal position expected on the basis of sp^2 hybridization at N1 and C8. Unfortunately, the crystal structure of the free ligand appears never to have been determined, precluding more detailed comparison.

The other features of the structure call for little comment, there being no exceptional angles or distances. The coordination geometry around Ir is octahedral, the CH bond occupying one vertex and the two hydride ligands, which may have been detected crystallographically but could not be refined, occupying two more. The P1–Ir–P2 angle of 165.0 (1)° is similar to the corresponding angle of 171.63 (8)° in **1**.[10] The overall geometry is similar, the mq having displaced the two acetone ligands of **1**.

Spectroscopic Characterization of the C–H···M Bridge. The IR spectrum of the mq complex **4a** shows a ν(C–H) stretch at 2848 cm^{-1} in the range[2] found for other C–H···M systems. This indicates a weakening of the C–H bond due to the interaction with the metal.

The ^1H NMR spectrum at −43 °C shows resonances expected for PPh_3, IrH_2, and mq. A resonance at δ −19.2 was assigned to IrH trans to N and at δ −28.6 trans to C–H···Ir. These are mutually coupled [^2J(H,H) = 8 Hz] and coupled to phosphorus [^2J(P,H) = 15 Hz]. Exchange between the CH_3 and IrH_2 was too slow to give significant magnetization transfer at accessible temperatures (≤30 °C).[11] Above −20 °C the hydride and mq methyl resonances are broad, which we ascribe to reversible loss of mq. A singlet at δ 1.1 is assigned to the mq methyl; even at −80 °C, the bridging and terminal C–H protons exchange rapidly. Isotopic perturbation of resonance[12a] can be used in such cases to confirm the asymmetric character of this group. Isotopic

(8) (a) On the basis of the usual covalent radii: Ir, 1.27 Å; C, 0.77 Å. (b) van der Waals radii: C, 1.6 Å; H, 1.2 Å; Ir 2.05 Å (estimated).
(9) Goodgame, D. L.; Hayman, P. B.; Riley, R. T.; Williams, D. J. *Inorg. Chim. Acta* **1984**, *91*, 89.
(10) Crabtree, R. H.; Hlatky, G. G.; Parnell, C. A.; Segmuller, B. E.; Uriarte, R. J. *Inorg. Chem.* **1984**, *23*, 354.
(11) Faller, J. W. In "Determination of Organic Structures by Physical Methods"; Academic Press, New York, 1973; Chapter 2. Sandstrom, J. "Dynamic NMR Spectroscopy"; Academic Press, New York, 1982.
(12) (a) Saunders, M.; Jaffe, M. H.; Vogel, P. *J. Am. Chem. Soc.* **1971**, *93*, 2558. Calvert, R. B.; Shapley, J. R.; Schulz, A. J.; Williams, J. M.; Snib, S. L.; Stucky, G. D. *Ibid.* **1978**, *100*, 6240. (b) **4a**: δ 8.15. Free 8-mq: δ 18.1.[12c] (c) Johns, S. R.; Willing, R. I. *Aust. J. Chem.* **1976**, *29*, 1617.

Table II. Positional and Anisotropic Thermal Parameters for **4a**[a]

atom	x	y	z	U_{11}	U_{22}	U_{33}	U_{12}	U_{13}	U_{23}
Ir1	0.0347 (0)	0.2417 (0)	0.8425 (0)	290 (2)	332 (2)	418 (2)	35 (2)	84 (1)	31 (2)
Sb1	0.1995 (1)	0.3255 (0)	0.4818 (1)	480 (6)	722 (7)	827 (7)	142 (5)	240 (5)	288 (5)
P1	0.0238 (1)	0.3441 (1)	0.9081 (2)	241 (17)	280 (15)	377 (15)	−23 (11)	59 (11)	5 (10)
P2	0.0229 (2)	0.1481 (1)	0.7317 (3)	329 (19)	291 (16)	451 (16)	40 (12)	124 (12)	29 (11)
F1	0.1261 (6)	0.3431 (6)	0.5557 (12)	1309 (99)	1580 (108)	1746 (113)	319 (82)	1072 (90)	4 (89)
F2	0.2725 (7)	0.3056 (5)	0.4058 (14)	1592 (110)	883 (76)	2584 (151)	388 (72)	1498 (111)	386 (86)
F3	0.2072 (5)	0.4091 (4)	0.4361 (11)	995 (77)	762 (64)	1907 (110)	360 (54)	673 (74)	543 (67)
F4	0.1939 (6)	0.2421 (5)	0.5282 (11)	1130 (81)	938 (75)	1789 (105)	25 (62)	578 (75)	614 (73)
F5	0.1349 (7)	0.3095 (7)	0.3332 (10)	1537 (111)	1883 (130)	1019 (84)	104 (97)	42 (77)	244 (84)
F6	0.2642 (7)	0.3388 (7)	0.6292 (11)	1356 (109)	2067 (144)	1299 (99)	−342 (100)	−500 (82)	198 (97)
N1	0.1503 (5)	0.2332 (4)	0.9143 (9)	274 (57)	517 (60)	616 (60)	7 (42)	90 (43)	−110 (46)
C2	0.1930 (7)	0.2532 (7)	0.8401 (12)	550 (105)	787 (103)	712 (86)	−133 (76)	277 (69)	1 (76)
C3	0.2669 (7)	0.2474 (8)	0.8804 (16)	206 (95)	1057 (131)	1401 (144)	−81 (83)	403 (86)	−31 (113)
C4	0.2974 (7)	0.2233 (8)	0.9916 (15)	194 (81)	1068 (128)	1149 (128)	129 (72)	−63 (74)	−139 (97)
C5	0.2877 (8)	0.1798 (8)	1.1834 (19)	433 (106)	748 (113)	1347 (160)	68 (78)	−150 (95)	130 (104)
C6	0.2473 (10)	0.1620 (8)	1.2608 (16)	851 (137)	731 (111)	893 (119)	1 (93)	−467 (95)	240 (90)
C7	0.1711 (8)	0.1679 (6)	1.2234 (11)	825 (112)	565 (87)	474 (73)	−176 (72)	−9 (67)	0 (58)
C8	0.1383 (6)	0.1885 (5)	1.1066 (10)	486 (79)	283 (60)	447 (63)	49 (48)	−65 (51)	−33 (45)
C9	0.1806 (6)	0.2087 (5)	1.0274 (10)	417 (79)	265 (58)	486 (67)	33 (47)	−73 (51)	−9 (44)
C10	0.2564 (7)	0.2044 (6)	1.0706 (12)	434 (90)	466 (77)	783 (91)	152 (59)	−82 (65)	69 (62)
C11	0.0584 (7)	0.1945 (6)	1.0750 (11)	575 (91)	744 (93)	580 (78)	29 (67)	227 (64)	310 (65)
C111	0.1067 (6)	0.3872 (5)	0.9711 (10)	393 (76)	429 (66)	417 (63)	−98 (50)	134 (51)	−64 (47)
C112	0.1574 (6)	0.3641 (6)	1.0709 (11)	412 (81)	539 (77)	521 (72)	−48 (56)	−25 (55)	−36 (55)
C113	0.2224 (7)	0.3953 (7)	1.1181 (13)	495 (95)	729 (98)	666 (89)	−28 (70)	−53 (67)	−27 (72)
C114	0.2324 (9)	0.4546 (9)	1.0739 (15)	678 (117)	1246 (149)	728 (106)	−504 (102)	−259 (84)	336 (99)
C115	0.1799 (10)	0.4817 (8)	0.9834 (16)	1110 (149)	866 (117)	999 (129)	−644 (103)	195 (110)	165 (94)
C116	0.1140 (8)	0.4495 (7)	0.9272 (14)	524 (100)	876 (109)	848 (105)	−320 (79)	200 (78)	77 (82)
C121	−0.0262 (5)	0.3946 (5)	0.7828 (10)	227 (68)	336 (61)	487 (66)	−19 (43)	47 (48)	77 (45)
C122	−0.0763 (6)	0.4379 (5)	0.8027 (10)	410 (78)	430 (69)	28 (52)	99 (53)	36 (50)	
C123	−0.1126 (7)	0.4776 (6)	0.7080 (12)	486 (88)	484 (76)	692 (85)	86 (57)	37 (64)	159 (60)
C124	−0.0980 (7)	0.4766 (6)	0.5960 (11)	713 (100)	565 (85)	420 (70)	38 (68)	−106 (61)	172 (57)
C125	−0.0464 (9)	0.4331 (7)	0.5742 (12)	1202 (141)	733 (104)	434 (80)	110 (92)	235 (81)	260 (68)
C126	−0.0114 (7)	0.3940 (6)	0.6689 (11)	707 (105)	598 (82)	526 (77)	107 (65)	343 (72)	97 (60)
C131	−0.0245 (5)	0.3510 (5)	1.0306 (9)	279 (67)	350 (59)	319 (54)	0 (43)	47 (42)	14 (39)
C132	−0.0861 (6)	0.3144 (5)	1.0207 (10)	358 (75)	424 (66)	475 (65)	97 (50)	181 (51)	55 (48)
C133	−0.1240 (7)	0.3199 (6)	1.1111 (13)	452 (90)	663 (89)	699 (89)	167 (66)	221 (67)	119 (69)
C134	−0.1019 (7)	0.3597 (6)	1.2103 (13)	660 (104)	682 (90)	711 (91)	−19 (71)	534 (78)	−122 (69)
C135	−0.0410 (8)	0.3953 (7)	1.2218 (12)	671 (105)	1036 (118)	512 (81)	177 (83)	314 (71)	222 (75)
C136	−0.0036 (6)	0.3909 (6)	1.1310 (11)	419 (84)	624 (81)	487 (70)	234 (60)	153 (57)	141 (57)
C211	0.1065 (6)	0.1059 (5)	0.7373 (10)	435 (78)	328 (63)	540 (69)	69 (49)	123 (54)	75 (48)
C212	0.1412 (7)	0.0780 (7)	0.8495 (13)	529 (96)	690 (94)	805 (97)	257 (70)	231 (74)	−48 (72)
C213	0.2058 (8)	0.0474 (8)	0.8622 (15)	532 (108)	1132 (135)	867 (116)	375 (90)	180 (87)	294 (96)
C214	0.2349 (9)	0.0444 (10)	0.7664 (21)	641 (137)	1422 (177)	1417 (185)	689 (119)	440 (126)	454 (141)
C215	0.2031 (12)	0.0746 (12)	0.6552 (20)	1338 (196)	2188 (261)	1164 (168)	1012 (187)	907 (152)	564 (170)
C216	0.1374 (9)	0.1055 (8)	0.6403 (15)	815 (124)	1240 (142)	929 (118)	576 (105)	633 (99)	357 (101)
C221	−0.0170 (5)	0.1575 (5)	0.5654 (10)	224 (68)	419 (66)	476 (63)	42 (46)	108 (47)	−44 (47)
C222	−0.0691 (7)	0.1157 (6)	0.4970 (12)	559 (91)	602 (85)	564 (79)	−123 (64)	43 (63)	93 (62)
C223	−0.0949 (8)	0.1262 (8)	0.3702 (14)	534 (101)	919 (117)	718 (98)	−204 (81)	−14 (74)	−160 (83)
C224	−0.0710 (7)	0.1706 (8)	0.3067 (12)	522 (96)	957 (116)	533 (82)	66 (79)	58 (65)	−48 (75)
C225	−0.0184 (8)	0.2102 (6)	0.3691 (12)	697 (103)	635 (89)	595 (84)	84 (71)	172 (71)	121 (64)
C226	0.0063 (7)	0.2044 (6)	0.4983 (11)	465 (83)	682 (85)	506 (73)	−39 (63)	86 (58)	−59 (60)
C231	−0.0316 (6)	0.0879 (5)	0.7820 (10)	461 (80)	279 (61)	499 (68)	−5 (48)	117 (53)	52 (45)
C232	−0.0837 (6)	0.1035 (6)	0.8411 (11)	414 (83)	526 (78)	533 (73)	31 (55)	109 (57)	31 (55)
C233	−0.1261 (7)	0.0574 (7)	0.8799 (12)	397 (89)	900 (112)	606 (84)	−107 (71)	270 (65)	160 (72)
C234	−0.1152 (8)	−0.0046 (7)	0.8521 (15)	592 (116)	624 (103)	933 (116)	−165 (76)	80 (86)	202 (81)
C235	−0.0657 (9)	−0.0216 (6)	0.7913 (17)	700 (121)	389 (84)	1486 (160)	44 (71)	506 (112)	192 (85)
C236	−0.0227 (7)	0.0237 (6)	0.7573 (15)	510 (97)	499 (84)	1096 (118)	1 (64)	323 (81)	82 (75)
H11	0.0459 (50)	0.1711 (44)	1.1285 (87)	380 (0)					
H12	0.0550 (50)	0.2355 (45)	1.0360 (90)	380 (0)					
H13	0.0351 (50)	0.1698 (45)	1.0086 (89)	380 (0)					

[a] Standard deviations given in parentheses.

perturbation has also been successfully applied to a number of other agostic systems.[2] In the case of a bridging methyl, the position of the RCH_2D resonance will differ substantially from that of RCH_3 if (a) the methyl group is in an environment sufficiently unsymmetrical to give different H/D ratios at different sites and (b) different sites differ in chemical shift. In the case of $RCH_2(\mu\text{-H})M$ the vibration frequencies of the terminal and bridging C–H groups differ sufficiently to affect the H/D ratio; D will prefer the terminal site because it has less zero point energy advantage in moving to the bridging site of lower force constant.

Deuterated **4a** does show the isotopic perturbation effect: the d_1 and d_2 mq methyl resonances are shifted by −0.14 and −0.28 ppm relative to the d_0 resonance. Structure A of Figure 1 can therefore be excluded, but B and C remain possibilities. That B is the true structure is shown by the absence of (<2 Hz) coupling between the mq methyl and PPh_3 as determined both by ^1H and by selective ^1H-decoupled ^{31}P NMR.

The magic-angle ^{13}C NMR spectrum of solid **4a**, kindly measured by Prof. K. Zilm, shows a −10 ppm coordination shift for the CH_3 group,[12b] the major part of which must be due to the formation of the C–H···Ir bridge.

Related Caffeine Complex. Caffeine gave a complex **4b** to which we assign a structure analogous to **4a**. The caffeine seems to be bound more strongly than mq, because the static ^1H NMR spectrum is observed even at room temperature. The addition of acetone and methanol caused no spectral change, but MeCN

Table III. Important Bond Angles (deg) and Distances (Å) for **4a**

Ir1–P1	2.314 (3)	C2–C3	1.38 (2)
Ir1–P2	2.312 (3)	C3–C4	1.33 (2)
Ir1–N1	2.168 (8)	C4–C10	1.38 (2)
Ir1–H12	2.08 (10)	C10–C9	1.42 (2)
Ir1–C11	2.69 (1)	C10–C5	1.35 (2)
Sb1–F1	1.84 (1)	C5–C6	1.35 (3)
Sb1–F2	1.86 (2)	C6–C7	1.42 (2)
Sb1–F3	1.86 (1)	C7–C8	1.36 (2)
Sb1–F4	1.85 (1)	C8–C9	1.40 (2)
Sb1–F5	1.82 (1)	P1–C111	1.82 (1)
Sb1–F6	1.81 (1)	P1–C121	1.82 (1)
H11–C11	0.85 (10)	P1–C131	1.83 (1)
H12–C11	0.96 (10)	P2–C211	1.82 (1)
H13–C11	0.92 (9)	P2–C221	1.82 (1)
C11–C8	1.49 (2)	P1–C231	1.82 (1)
N1–C2	1.37 (2)		
N1–C9	1.34 (1)		
P1–Ir1–P2	165.0 (1)	Ir1–H12–C11	119 (8)
P1–Ir1–N1	97.3 (2)	C11–C8–C9	123.4 (9)
P1–Ir1–H12	75.2 (27)	C11–C8–C7	117.0 (12)
P2–Ir1–N1	94.5 (3)	C8–C7–C6	120.1 (14)
P2–Ir1–H12	117.3 (26)	C7–C6–C5	120.4 (14)
N1–Ir1–H12	73.0 (27)	C6–C5–C10	120.2 (14)
F1–Sb1–F2	178.5 (4)	C5–C10–C4	120.5 (13)
F1–Sb1–F3	92.8 (5)	C5–C10–C9	121.3 (14)
F1–Sb1–F4	88.0 (5)	C9–C10–C4	118.1 (11)
F1–Sb1–F5	90.9 (6)	C10–C4–C3	120.9 (12)
F1–Sb1–F6	89.8 (6)	C4–C3–C2	120.7 (16)
F2–Sb1–F3	88.4 (5)	C3–C2–N1	120.2 (12)
F2–Sb1–F4	90.8 (5)	C2–N1–C9	119.6 (9)
F2–Sb1–F5	88.2 (6)	N1–C9–C10	120.4 (11)
F2–Sb1–F6	91.1 (6)	N1–C9–C8	121.0 (10)
F3–Sb1–F4	178.8 (5)	C8–C9–C10	118.4 (10)
F3–Sb1–F5	90.8 (5)	C7–C8–C9	119.3 (11)
F3–Sb1–F6	90.8 (6)		
F4–Sb1–F5	90.0 (6)		
F4–Sb1–F6	88.4 (6)		
F5–Sb1–F6	178.3 (11)		

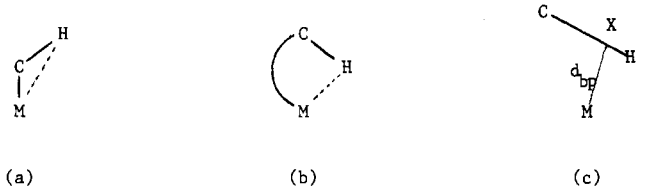

Figure 3. Different types of C–H···M systems and the definition of d_{bp}. Some systems (a) such as agostic methyl groups have the C–H carbon also directly bonded to M, with the C–H pointing away from the metal. Other systems such as **4** have the C–H carbon only indirectly linked to the metal via a chain of other atoms, and the C–H bond tends to point toward M (see b). The definition of d_{bp} (see c) can be applied to both classes of bridged systems.

displaced the caffeine bridging methyl to give $[IrH_2(MeCN)(caff)L_2]^+$.

Structural Comparison of Known C–H–M Systems. Some 17 structures containing C–H–M bridges have been reported in which all three atoms of the bridge have been located.[13-26] In some of these, the carbon is also directly bound to the metal (Figure 3a). In other cases, as here, this carbon is also bound to other atoms of the ligand (Figure 3b). The M–C distance can be longer or shorter than the M–H distance because the C–H vector can point toward (b) or away (a) from the metal. We wanted to be able to use a single structural parameter to characterize the strength of the C–H to metal interaction in all the known cases. M–C or M–H distances taken in isolation are not directly comparable because of the different directions in which the C–H vector can point.

It is the pair of C–H bonding electrons that forms the new bond to the metal, and so we consider as most significant, not the M–C nor M–H distances, but the distance d_{bp} from the metal to this C–H bonding electron pair. Carbon and hydrogen have much the same electronegativity,[27] so we consider the bonding pair to be located on the C–H vector at the point (X in Figure 3c) where the covalent radii of C and H meet. Simple formulas (eq 3 and 4) involving the three distances d_{MH}, d_{MC}, and d_{MH} and a constant

$$d_{bp} = [d_{MH}^2 + r^2 d_{CH}^2 - r(d_{MH}^2 + d_{CH}^2 - d_{MC}^2)]^{1/2} \quad (3)$$

$$H = \cos^{-1}\left\{\frac{d_{CH}^2 + d_{MH}^2 - d_{MC}^2}{2 d_{CH} d_{MH}}\right\} \quad (4)$$

r give d_{bp}, the distance required (see supplementary material for derivation), and H, the angle M–H–C. The constant r (=0.28) is the ratio of the H covalent radius to the standard C–H distance (1.09 Å).

C–H bond lengths obtained in X-ray work are ca. 0.1 Å[28] shorter than the true internuclear separation as given in neutron work. For this reason, l_{MH} and l_{CH} obtained from X-ray data must be corrected by applying eq 5 and 6 (see supplementary material for derivation) before eq 3 and 4 can be used.

$$d_{MH} = l_{MH} + 0.1\left\{\frac{l_{CH}^2 + l_{MH}^2 - d_{MC}^2}{2 l_{CH} l_{MH}}\right\} \quad (5)$$

$$d_{CH} = l_{CH} + 0.1 \quad (6)$$

The d_{bp} so obtained is a measure of the degree of C–H to metal interaction. In order to make data from metals of different covalent radii comparable, however, r_M, the covalent radius of the metal, must be subtracted (eq 7). The resulting value, r_{bp}, is

$$r_{bp} = d_{bp} - r_M \quad (7)$$

effectively the covalent radius of the C–H bonding electrons. If r_{bp} is large, the bridging interaction is weak; if small, it is strong.

Values of r_{bp} and H (the angle M–H–C) appear in Table IV for all the reported cases of C–H···M bridged structures. The most striking feature of the results is the very great range of r_{bp}. For the lowest values, 0.4–0.5 Å, both d_{MC} and d_{MH} distances are essentially the same as observed for single M–C and M–H covalencies. For values of r_{bp} greater than ca. 1.9 Å, d_{MH} and d_{MC} become indistinguishable from distances appropriate to simple van der Waals contacts. The observed values of r_{bp} are roughly evenly spread between these extreme values, a striking illustration of the structural variability of the C–H···M system.

(13) Otsuka, S.; Yoshida, T.; Matsumoto, M.; Nakatsu, K. *J. Am. Chem. Soc.* **1976**, *98*, 5850.
(14) LaPlaca, S. J.; Ibers, J. A. *Inorg. Chem.* **1965**, *4*, 778.
(15) Kuzinina, L. G.; Strukhov, Y. T. *Cryst. Struct. Commun.* **1979**, *8*, 715.
(16) Roe, D. M.; Bailey, P. M.; Moseley, K.; Maitlis, P. M. *J. Chem. Soc., Chem. Commun.* **1972**, 1273.
(17) Cotton, F. A.; LaCour, T.; Stanislowksi, A. J. *J. Am. Chem. Soc.* **1974**, *96*, 754.
(18) Dawoodi, Z.; Green, M. L. H.; Mtetwa, V. S. B.; Prout, K. *J. Chem. Soc., Chem. Commun.* **1982**, 802 and 1410.
(19) Carmona, E.; Sanchez, L.; Marin, J. M.; Poveda, M. L.; Atwood, J. L.; Priester, R. D.; Rogers, R. D. *J. Am. Chem. Soc.* **1984**, *106*, 3214.
(20) Brown, R. K.; Williams, J. M.; Schultz, A. J.; Stucky, G. D.; Ittel, S. D.; Harlow, R. L. *J. Am. Chem. Soc.* **1980**, *102*, 981.
(21) Schultz, A. J.; Teller, R. G.; Beno, M. A.; Williams, J. M.; Brookhart, M.; Lamanna, W.; Humphrey, M. B. *Science (Washington, D.C.)*, in press.
(22) Schultz, A. J.; Williams, J. M.; Schrock, R. R.; Rupprecht, G. Fellmann, J. D. *J. Am. Chem. Soc.* **1979**, *101*, 1593.
(23) Dawkins, G. M.; Green, M.; Orpen, A. G.; Stone, F. G. A. *J. Chem. Soc., Chem. Commun.* **1982**, *41*.
(24) Schultz, A. J.; Brown, R. K.; Williams, J. M.; Schrock, R. R. *J. Am. Chem. Soc.* **1981**, *103*, 169.
(25) Green, M.; Norman, N. C.; Orpen, A. G. *J. Am. Chem. Soc.* **1981**, *103*, 1269.
(26) Tachikawa, M.; Muetterties, E. L. *J. Am. Chem. Soc.* **1980**, *102*, 4541.
(27) Pauling, L. "The Nature of the Chemical Bond", 3rd ed.; Cornell University Press: Ithaca, NY; 1960.
(28) (a) This is only an approximation and might differ for different metals, but it was thought better to use one value throughout to avoid possible bias in the final results. (b) Teller, R. G.; Bau, R. *Struct. Bonding (Berlin)* **1981**, *44*, 1. (c) The true hydrogen atom position is taken as lying on the CH vector as determined by X-ray methods and 0.1 Å beyond the X-ray position for the hydrogen atom.

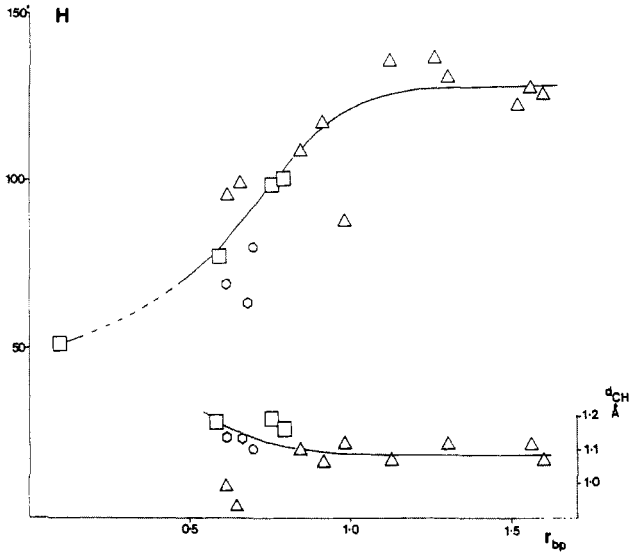

Figure 4. Plot of both H (the angle C–H–M in deg) and d_{CH} (Å) against r_{bp} (Å) from Table IV. Squares and hexagons refer to neutron data, triangles and circles to X-ray data. Hexagons and circles refer to α-CH bridges that are more constrained geometrically than β and higher types (squares and triangles); more weight is attached to the latter, particularly with regard to H. Only when r_{bp} falls appreciably below 1.0 does H fall below 130° and d_{CH} rise significantly above the value in the free C–H bond (ca. 1.08 Å). The calculated value of H for a cis alkyl hydride complex (entry 21 of Table IV) is also included; the corresponding value of d_{CH} (2.68 Å) is too large to include in this plot.

The most strongly interacting group of complexes in Table IV (r_{bp} < 0.7 Å) consists of a number of cluster complexes, Schrock's[22,24] alkylidenes **16** and **18** and Green's[18] agostic methyl **15**. The next group (0.7 Å > r_{bp} > 1.0 Å) consists of a group of five mononuclear structures, including our own Ir case. The weakly interacting cases have r_{bp} > 1.0 Å and tend to involve the later transition metals. It can also be seen that as r_{bp} becomes smaller, d_{CH} increases. That is to say that C–H bond is weakened as the interaction with the metal increases. The angle H also falls off with decreasing r_{bp}.

We have found no cases in which r_{bp} is less than 1.9 Å in an 18-electron metal complex. This shows that the C–H bond is not close to the metal simply by accident but that the 2-electron deficiency at the metal is *required* for bridging to occur. This requirement for electron deficiency suggests that both lanthanide and actinide complexes and metal surfaces, all having electron deficiency, will readily give C–H-bridged structures.

Bürgi and Dunitz[29] have shown that a succession of static X-ray structures can give information about the dynamics of a reaction. Each structure is considered to be a point on the reaction profile frozen for detailed examination. It may seem unlikely that information about the thermodynamically most stable arrangements of atoms in a given progession of crystal structures could give information about the corresponding reaction profile, a kinetic phenomenon. In fact it is not so unreasonable that the deformation of a group of atoms, under different constraints in different structures, should adopt geometries corresponding, approximately at least, to the "valley floor" of the reaction hypersurface that leads up to the transition state in the unconstrained system. Many recent applications of the methods have led to results strikingly in agreement with theoretical and other experimental evidence and so lend credence to the method. We have therefore plotted d_{CH} and the angle H (M–H–C) against r_{bp} (Figure 4). This shows that early in the "reaction" (r_{bp} large) M–H–C is ca. 130°, but that on approaching the metal the C–H bond rotates so as to close the angle down to ca. 95° at r_{bp} = 0.4 Å. Smooth curves for H and d_{CH} have been drawn through the experimental points of Figure 4. The product of the oxidative addition, a cis alkyl hydride complex has also been included on the diagram, assuming normal

(29) Bürgi, H. B.; Dunitz, J. D. *Acc. Chem. Res.* **1983**, *16*, 153.

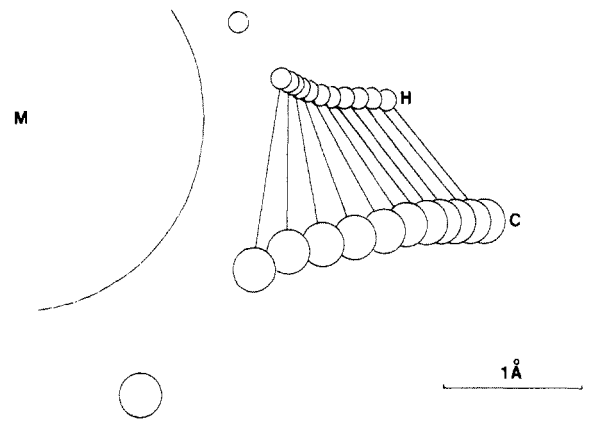

Figure 5. The C–H + M → C–M–H trajectory as defined by the curves plotted in Figure 4. The large curve corresponds to the surface of the metal atom as defined by the covalent radius of the metal. The smaller circles represent carbon and hydrogen atoms but are drawn with arbitrary radii smaller than the corresponding covalent radii, for clarity. The straight lines joining the C and the H atoms are the successive positions of the CH internuclear vector on varying r_{bp} by increments of 0.1 Å. The isolated circles are the final positions of the carbon and hydrogen atoms expected for a cis alkyl hydride complex, assuming normal M–C and M–H distances and an angle of 90° for C–M–H. The resulting trajectory shows the C–H bond approaching the metal, with the C–H vector pointing toward the metal and with an M–H–C angle of ca. 130°. The C–H bond then rotates and elongates before finally breaking. Some inferences based on this course of events are discussed in the text.

Figure 6. Possible bonding interactions between a C–H bond and a transition metal in a bridging C–H···M system. In what we have called the σ bond, an empty d orbital accepts electron density from the C–H bond by overlap with the H (1s) and C (sp^3) orbitals (see a). In b, back-donation from a filled d orbital to the σ^* orbital of the C–H system is illustrated.

bond lengths and a 90° H–M–C angle for a typical octahedral complex. These curves probably approximately describe the trajectory for a C–H bond approaching a metal. This has been represented pictorially in Figure 5 by plotting successive positions of the C–H bond as r_{bp} is decreased stepwise by 0.1 Å over the range 1.6–0.4 Å. The position and orientation of each successive C–H bond position are completely defined by constraining the direction of the r_{bp} vector to be horizontal in each case. It can be seen that r_{bp}, which corresponds to a reaction coordinate, falls to 0.05 Å in the product alkyl hydride.

The resulting profile is chemically reasonable. The C–H bond approaches the metal and gradually swings round and elongates until it is cleaved. Both carbon and hydrogen atoms follow a smooth trajectory to the final alkyl hydride product.

The orientation of the C–H bond at large r_{bp} may be significant. The value of H is ca. 130° not 180°, as would be consistent with steric repulsion between the metal and the other groups on carbon. This might be an artefact due to the inability of any of the structures studied to achieve H = 180°. Examination of models, however, suggests that in many cases the bridging C–H bond could easily rotate to increase H substantially, if not all the way to 180°. The orientation observed may therefore also apply to the approach of a C–H bond in a free substrate molecule such as an alkane. An H of 130° might be favored for the following reasons. The metal is accepting a C–H bonding pair of electrons into an empty d_σ orbital. This d_σ orbital can therefore maximize its interaction with the C–H bonding pair by overlap with both the H 1s and with the C sp^3 hybrid (Figure 6a) components of the C–H σ bond. An off-axis approach may be favored because it maximizes both

M–H and M–C interaction. A similar explanation has been proposed[28b] to account for the nonlinearity of M–H–M bridges, which are formed by interaction of an M–H bond (rather than a C–H bond) with a 16-electron metal.

The second factor that might favor an off-axis approach ($H < 180°$) is the availability of the C–H σ^* orbital for back-donation from the filled d_π metal orbitals only for off-axis geometry (Figure 6b). These d_σ and d_π interactions are entirely analogous to the σ and π components of a metal–CO bond except that the nature of the ligand orbitals differs. Both σ and π components serve to weaken the C–H bond. At large r_{bp} the π component may predominate because the C–H σ^* orbital, which extends beyond the H atom toward the metal, is more accessible for overlap with the metal than is the C–H σ orbital at this distance. The importance of the σ^* orbital in C–H and H–H activation has been emphasized before,[30,31] particularly by Saillard and Hoffmann.[32] At smaller r_{bp} the CH bond rotates to become more broadside-on, by which time the σ interaction is probably as strong or stronger than the π. The σ^* effect does not always contribute, because in several cases d^0 metal complexes also contain C–H···M bridges.

Interestingly, Sevin[30] has proposed, on theoretical grounds, a trajectory for H_2 + M that resembles the CH + M trajectory discussed above in the sense that the H_2 first approaches end-on ($H = 180°$) and then swings round. We, too, have discussed such an approach previously,[5,31] and several workers[32] have considered in detail the theoretical implications of C–H and H–H additions to metals.

Reductive elimination of H_2 from MH_2 or of CH_4 from M(H)(CH_3) must go by the reverse of the oxidative-addition mechanism. If the picture we suggest is true, some of the heat of reaction may appear as excess rotational energy in the products. The picture might therefore be testable in molecular beam experiments.

About 1.2 Å of the carbon and 0.5 Å of the hydrogen trajectories appear as gaps in Figure 5. These gaps may correspond to the activation barrier of the C–H + M → C–M–H process. The transition state probably lies in this gap, perhaps quite close to the last C–H bond position shown.[7] It can be seen that the M–C and M–H bonds are probably formed to a substantial extent before transition state is reached; the main activation barrier probably involves breaking the C–H bond and rehybridizing the carbon. This rehybridization is evident from an examination of angular deformations in the crystal structural data for molecules of small r_{bp}, but the situations are so varied that it was not possible to express this effect in terms of a single comparable parameter. Insufficient data are as yet available to allow useful comparison of r_{bp} with $^1J(^{13}C–H)$ or ν(C–H), but a correlation is to be expected.

Stability of C–H···M Bridges. Why does complex **4** not spontaneously rearrange to a cyclometalated form such as [Ir(N⌒CH_2)H_3L_2]$^+$ (**23**) or [Ir(N⌒CH_2)HL_2]$^+$ (**24**, N⌒CH_2 = 8-methylquinolinyl)? **23** would be an unusual example of Ir(V), and **24** would be Ir(III) but 16-electron, and both species are probably involved in the H/D exchange chemistry mentioned above. Both **23** and **24** are apparently less stable than **4**, however. Perhaps, as Halpern[33] has argued, the explanation is that the Ir–C bond is insufficiently strong to favor **23** or **24** with respect to **4**.

Figure 4 shows that the C–H bond length is little affected by coordination until r_{bp} falls below 0.8–0.9 Å, suggesting that the C–H bond dissociation energy falls little on forming the bridge. Clearly, the CH–M bond energy outweighs the drop in the C–H bond energy to make the C–H···M structure thermodynamically stable with respect to the isolated C–H bond and 16-electron metal fragment.

In the case of d^0 metals, it is easier to understand why cyclometalation does not occur. In this case the metal cannot tolerate an oxidative addition, although with a suitable leaving group, heterolytic C–H activation can still occur.

Inter- vs. Intramolecular C–H Activation. One of the questions in the field of alkane activation is why certain systems break C–H bonds even in alkanes but ignore the C–H bonds of their own ligands. In the case of our own work[5] one would argue that the formation of a stable dehydrogenation product provides a thermodynamic sink that is able to reverse any cyclometalation side equilibrium. Even so, very little deuterium is found in the PPh_3 ligands when C_6D_{12} is dehydrogenated.[5] The systems of Bergman,[34] Graham,[35] Jones,[36] and Watson,[37] involving as they do simple C–H activation, cannot be understood in this way. Cyclometalation is either (a) thermodynamically or (b) kinetically unfavorable in these cases. If cyclometalation were thermodynamically disfavored, it might be possible to make the cyclometalated product independently and show that it reacts with alkanes. However, hundreds of cyclometalated species are known,[3] and none have been reported to activate alkanes. Efforts to synthesize an ortho-metalated analogue of **1** have failed. Interestingly, Jones et al.[36b] have shown[3] that (C_5Me_5)Rh(PMe_2-*n*-Pr)H_2, on photolysis, *does* give a cyclometalated product in competition with intermolecular C–H activation of propane; in this case they have shown that cyclometalation is thermodynamically favored but kinetically disfavored. This may well point the way to a solution of the problem, but we still need to know the physical origin of these effects. The trajectory arguments discussed above suggest a possible reason why cyclometalation might be kinetically disfavored compared to reaction with the alkane in this and other systems. If the C–H bond must approach in a certain orientation to be cleaved, then failure to attain this orientation could kinetically inhibit reaction. Examination of models shows that the C–H bonds of PPh_3, PMe_3, and C_5Me_5 cannot readily follow the C–H + M trajectory of Figure 5 without strain. On the other hand, as the R groups of PR_3 become longer, the ends of the chain become freer to adopt any required geometry. That conformational effects can influence the reactivities of organometallic compounds is well-known and has been illustrated in Whitesides'[38] study on the requirement for MCCH coplanarity for β-elimination and our own similar conclusion[39] in the case of the reverse reaction, olefin insertion.

If this is so, why do the majority of metal complexes cyclometalate rather than activate alkanes? We believe that the balance between the two reactions is decided by the opposing effects of the conformational effect, mentioned above, and steric congestion of the complex. As shown by Shaw,[39b] steric congestion strongly accelerates cyclometalation, no doubt because the degree of congestion tends to fall on the approach to the transition state. For alkane activation, in contrast, congestion increases, because an external reagent is involved. This suggests that complexes with a lesser degree of congestion should tend to activate alkanes rather than cyclometalate. All the successful PPh_3-based systems are of the uncongested ML_2 variety.[1] (C_5Me_5)ML systems, more congested, cyclometalate with PPh_3 and require the inherently more metalation-resistant PMe_3 to give exclusive reaction with alkanes.[34] Alkane activation is rare, not because it is unfavorable kinetically, but because deactivation reactions such as cyclometalation tend to divert the course of the reaction. Identifying and preventing these reactions will be a key element for further advance in catalytic alkane activation chemistry.

Steric Effects and Selectivity in Alkane Activation. The trajectory of Figure 5 also casts light on the steric effects to be expected in alkane C–H activations. In general, the presence of both bulky substituents on the carbon of the C–H bond to be

(30) Sevin, A. *Nouv. J. Chim.* **1981**, *5*, 233.
(31) Crabtree, R. H.; Quirk, J. M. *J. Organomet. Chem.* **1980**, *199*, 99.
(32) Saillard, J. Y.; Hoffman, R. *J. Am. Chem. Soc.* **1984**, *106*, 2006. See also: Shustorovich, E. *J. Phys. Chem.* **1983**, *87*, 14.
(33) Halpern, J. *Acc. Chem. Res.* **1982**, *15*, 238.
(34) Bergman, R. G.; Janowicz, A. H. *J. Am. Chem. Soc.* **1982**, *104*, 352.
(35) Hoyano, J. K.; Graham, W. A. G. *J. Am. Chem. Soc.* **1982**, *104*, 3743.
(36) Jones, W. D.; Feher, F. J. *J. Am. Chem. Soc.* **1982**, *104*, 4240.
(37) Watson, P. L. *J. Am. Chem. Soc.* **1983**, *105*, 6491.
(38) McDermott, J. X.; White, J. F.; Whitesides, G. M. *J. Am. Chem. Soc.* **1976**, *98*, 6521. See also: Shaw, B. L. *Chem. Commun.* **1968**, 464.
(39) (a) Crabtree, R. H.; Felkin, H.; Fillebeen-Khan, T.; Morris, G. E. *J. Organomet. Chem.* **1979**, *168*, 183. (b) Cheney, A. J.; Shaw, B. L. *J. Chem. Soc., Dalton Trans.* **1972**, 754.

Table IV. Experimental Data for Complexes **4–20** and Derived Values of r_{bp} and H

no.	complex[a]	type[b]	data[c]	l_{MH} or d_{MH},[d] Å	d_{MC}, Å	l_{CH}[d] or d_{CH}, Å	d_{bp}, Å	r_{bp}, Å	H, deg	ref
5	$[Pt(PPh_2\text{-}t\text{-}Bu)_2]_2$	γ	X	2.77	3.45	0.97	2.9	1.6	126	13
6	$[Pd(PPh_2\text{-}t\text{-}Bu)_2]_2$	γ	X	2.70	3.46	1.05	2.84	1.56	128	13
7	$RuCl_2(PPh_3)_3$	γ	X	2.59	3.314	{1.09}	2.79	1.52	123	14
8	$Pt(PhCHNMe)_2Cl_2$	δ	X	2.44	3.22	1.01 (5)	2.59	1.3	131	15
9	$Pd(C_4Me_4)(PPh_3)Br$	δ	X	2.31	3.19	{1.08}	2.54	1.26	137	16
10	$Mo(Et_2B(pz)_2)(\eta^3\text{-}PhC_3H_4)(CO)_2$	ϵ	X	2.27	3.06	0.97	2.42	1.12	136	17
11	$TiEtCl_3(dmpe)$	β	X	2.29	2.516	1.02	2.30	0.98	88	18
4	$[IrH_2(mq)L_2]A$	δ	X	2.08	2.69	0.96	2.18	0.91	117.5	this work
12	$Mo(OAc)(dtc)(CO)L_2$	β	X	2.06	2.60	1.00	2.14	0.84	109	19
13	$[Fe(\eta^3\text{-}C_8H_{13})(P(OMe)_3)_3]A$	β	N	1.874	2.384	1.164	1.96	0.79	101	20
14	$Mn(\eta^3\text{-}C_6H_8Me)(CO)_3$	β	N	1.84	1.19	2.34	1.92	0.75	99	21
15	$TiMeCl_3(dmpe)$	α	X	2.03	2.149	1.00	2.01	0.69	80	18
16	$Ta(CH\text{-}t\text{-}Bu)LCl_3$	α	N	2.119	1.898	1.131	2.00	0.68	63	22
17	$[Fe_2Cp_2(CO)(dppm)Me]A$	β	X	1.78	2.118	0.83	1.82	0.65	99	23
18	$TaCp^*(CH\text{-}t\text{-}Bu)(C_2H_4)L$	α	N	2.043	1.946	1.135	1.95	0.61	69	24
19	$[Mo_2Cp_2(C_{11}H_{15})]A$	β	X	1.88	2.196	0.89	1.91	0.61	96	25
20	$Fe_4(CH)(H)(CO)_{12}$	α	N	1.80	1.926	1.18	1.76	0.59	77	26
21	*cis*-$Ir(Me)(H)L_n$			{1.7}	{2.07}	{2.679}	1.35	0.05	51	this work
22	$Ir(CH_4)$ vdW contact			{2.9}	{3.569}	{1.09}	3.06	1.79	119	this work

[a] pz = pyrazolyl, dmpe = $Me_2PCH_2CH_2PMe_2$, mq = 8-methylquinoline, dtc = Et_2NCS_2, dppm = $Ph_2PCH_2CH_2PPh_2$, Cp* = $\eta^5\text{-}C_5Me_5$. See the original references for further details. [b] α if the bridging H is attached to an atom α to the metal. [c] X-ray or neutron data. [d] The true internuclear distances as obtained from neutron data are d_{XY}, but the observed distances from X-ray data are l_{MH} and l_{CH} and have to be corrected (see text). Estimated values are enclosed in braces.

cleaved and lack of conformational flexibility would both be expected to hinder the C–H cleavage. As Felkin et al.[40] have shown, attack at the methyl group of methylcyclohexane is preferred over attack at any other position; in the case of the $ReH_7(PPh_3)_2$/*tert*-butylethylene system, attack at the 1- or 2-positions on the ring is least favored, in spite of the fact that this could give the most thermodynamically stable of the possible product olefins after β-elimination. The same effects may help disfavor attack of the metal on C–H bonds of a second molecule of complex. Saillard and Hoffman[32] have previously emphasized the importance of steric effects in C–H activation.

Conclusion. We have shown that C–H···M-bridged species can be formed in the "$IrH_2L_2^+$" system, as also found by Morris,[6] and that they can lead to selective catalytic H/D exchange in the substrate. We have also systematized the structural data on all the known bridged systems and have suggested a C–H + M → C–M–H reaction trajectory. This has lead to a possible explanation of the preference for reaction with alkane, rather than ligand C–H bonds, in the known alkane activation systems.

Experimental Section

Reagents. Ammonium chloroiridate was a gift of Johnson Matthey, Inc. Ligands were purchased from Aldrich Chemical Co.

Spectroscopy. NMR spectra were recorded on Bruker 270 MHz instrument, and shifts are reported in ppm relative to Me_4Si. IR spectra were recorded on a Nicolet 7000 Series FT IR instrument.

Syntheses. Starting materials were prepared by published procedures.

Dihydrido(η^3-8-methylquinoline-*N*,*C*,*H*)bis(triphenylphosphine)iridium(III) Salts. $[Ir(cod)(PPh_3)_2]A$ salts (A = BF_4, PF_6, SbF_6; 0.2 mmol) in CH_2Cl_2 (10 mL) were treated with 8-methylquinoline (30 mg, 0.21 mmol), cooled to 0 °C, and treated with H_2 (1 atm) for 40 min. The volume of the solution was reduced to 5 mL in vacuo, and diethyl ether (25 mL) was added to precipitate the white product, yield 80%. Recrystallization from CH_2Cl_2/Et_2O gave the analytically pure material. Anal. Calcd for $C_{46}H_{47}IrP_2F_6N\cdot0.33CH_2Cl_2$: C, 53.75; H, 4.05; N, 1.35. Found: C, 53.56; H, 4.31; N, 1.29. The complexes in which A = BF_4 and SbF_6 were analogous spectroscopically to the PF_6 complex and were not analyzed.

The caffeine complex was prepared by a similar method (A = BF_4); yield 83%. Anal. Calcd for $C_{44}H_{42}P_2N_4O_2BF_4Ir\cdot{}^2/_3CH_2Cl_2$: C, 50.78; H, 4.20; N, 5.30. Found: C, 50.82; H, 4.59; N, 5.12. IR: ν(Ir–H) = 2180 cm^{-1}. NMR (270 MHz, CD_2Cl_2, 220 K): δ −29.3 (dt 8, 15, IrH trans to C–H··Ir), −22.3 (dt, 8, 15, IrH trans to N), 3.64, 3.12, (6 H), s, Me), 7.39–7.6 (c, aromatic).

Crystallographic Data Collection and Refinement. A pale yellow prism of $[IrH_2(mq)L_2]SbF_6$ was sealed in a capillary and mounted on a Syntex P3 automated diffractometer. The unit cell (Table I) was determined from 15 independent reflections ($2\theta > 15°$) with Mo Kα (λ = 0.71069 Å) radiation. Data (8055 points) were collected at room temperature by a variable scan rate, θ–2θ scan mode, and a scan width of 1.2° below Kα_1 and 1.2° above Kα_2 to a maximum 2θ of 116°. Backgrounds were measured each side of the scan for a combined time equal to the total scan time. The intensities of three standard reflections were measured every 97 reflections, and as they showed less than 6% variation, no correction for decomposition was performed. Data were corrected for Lorentz, polarization, and background effects. Transmission factors were calculated based on a ψ scan, and as the range was small (0.95–1.00), the crystal being regular (0.15 × 0.15 × 0.25 mm), the absorbtion correction was not applied. After removal of redundant data and forbidden reflections, 4749 were considered observed ($I > 3\sigma(I)$). The structure was solved by a Patterson synthesis to locate the Ir and Sb atoms. Successive least-squares/difference Fourier cycles allowed location of the non-hydrogen atoms. Refinement for scale factor and positional and anisotropic thermal parameters was carried out to convergence.[41] All the hydrogen atoms were detected in a difference Fourier synthesis. The three hydrogens of the mq methyl group (C11) were stable to refinement, and their positions are reported. The aromatic hydrogen positions were not refined but were included in F_c, and the IrH_2 hydrogens were not stable to refinement, and their positions are not reported. The aromatic hydrogens were assigned isotropic thermal parameters of U = 0.03 Å^2 and all associated parameters held constant. The final cycle of refinement [function minimized $\sum(|F_o| - |F_c|)^2$] led to a final agreement factor of R = 4.6% [$R = 100(\sum(||F_o| - |F_c||)/|F_o|)$]. Anomalous dispersion corrections were made for Sb and Ir, and scattering factors were taken from Cromer and Mann.[42] Unit weights were used throughout.

Acknowledgment. We thank Professor W. D. Jones for communicating some of his results prior to publication, Professor H. D. Kaesz for helpful discussions, the NSF for support, and Johnson Matthey, Inc., for a loan of iridium. R.H.C. thanks the Camille and Henry Dreyfus Foundation for a Fellowship. We are also particularly grateful to Prof. K. Zilm for obtaining a solid-state NMR spectrum.

Registry No. **1**, 24419-58-7; **3** (A = BF_4), 38834-40-1; **3** (A = PF_6), 61817-47-8; **3** (A = SbF_6), 91410-27-4; **4a** (A = PF_6), 96394-22-8; **4a** (A = BF_4), 96394-23-9; **4a** (A = SbF_6), 96411-83-5; **4b** (A = BF_4), 96394-25-1; **5**, 96394-26-2; **6**, 96394-27-3; **7**, 15529-49-4; **8**, 96394-28-4; **9**, 96394-29-5; **11**, 96443-80-0; **13**, 66060-15-9; **15**, 85944-68-9; **20**, 76547-44-9; mq, 611-32-5; caff, 58-08-2; 2-methylquinoline, 91-63-4.

Supplementary Material Available: Tables of structure factors, additional distances and angles, and hydrogen atom positions and a derivation of eq 3–6 (48 pages). Ordering information is given on any current masthead page.

(40) Baudry, D.; Ephritikine, M.; Felkin, H.; Holmes-Smith, R. *Chem. Commun.* **1983**, 788.

(41) Stewart, J. M., Ed. "The X-ray System Version of 1980", Technical Report No. TR 446; Computer Center, University of Maryland: College Park, MD, 1980.

(42) Cromer, D. T.; Mann, J. B. *Acta Crystallogr., Sect. A: Cryst. Phys., Diffr., Theor. Gen. Crystallogr.* **1961**, *A24*, 321.